Photonics Based on Wavelength Integration and Manipulation
IPAP Books 2 (2005) pp. 101–112

Development of Rare-Earth Doped Fiber Amplifiers for Broad Band Wavelength-Division-Multiplexing Telecommunication

Setsuhisa TANABE

Graduate School of Human and Environmental Studies, Kyoto University,
Sakyo-ku, Kyoto 606-8501, Japan

Rare-earth-doped novel oxide glass and glass ceramic materials for optical amplifiers were developed for WDM telecommunication and their spectroscopy and local structure were investigated. In a series of Er-doped glasses with broad 1.5μm emission, heavy-metal oxide glasses were found to offer specific local environment to Er^{3+} ions. Potential of nano-glass ceramics for U-band amplifier is shown in a YAG precipitated silicate glass ceramic materials. Also, spectroscopic studies on optical properties of Tm^{3+}-doped tellurite glasses are presented as candidate materials of S-band amplifier. The Judd-Ofelt analysis showed 96% quantum efficiency of 1.46μm transition in a tellurite host, which has properties superior to fluoride fibers. Various possibilities of broadband amplifier materials in the system of rare-earth doped glasses are presented.

KEY WORD: optical amplifier, rare-earth, glass, erbium, thulium, optical fiber, telecommunication

1. Introduction

Due to rapid increase of information traffic and the need for flexible networks, there exists urgent demand for optical amplifiers with a wide and flat gain spectrum in the telecommunication window, to be used in the wavelength-division-multiplexing (WDM) network system[1)]. After the invention of the Er-doped fiber amplifier (EDFA), various types of amplifier devices have been developed in order to broaden the telecommunication bandwidth in the WDM network[P1]. Tm^{3+}-doped and Pr^{3+}-doped fluoride fiber amplifiers have been developed for the S-band and O-band applications, respectively. Long-term reliability of fluoride fibers is still an issue for practical use[P2]. The Raman amplifier composed of conventional silica fiber is also becoming practical use in WDM system that requires small gain (~10dB) in broad wavelength range. The gain range and bandwidth can be controlled by the wavelength and configuration of pumps. However, the pump power required is very high compared with the rare-earth doped fiber amplifiers. Still the rare earth doped amplifiers can be promising in the practical system due to their high power conversion efficiency.

Most of the EDFA utilized at present is made of silica-based glass fiber, where doped Er^{3+} ions show narrow emission band at 1.55μm resulting in narrow gain spectra. Following the report of wide spectra[2)], Mori reported excellent performance of a tellurite based EDFA[3)], which shows 80nm-wide gain around 1.53 ~ 1.61μm. In order to increase the channels and to improve the performance of WDM network, it is important to investigate a material with wider gain spectra. We have reported that the Bi_2O_3-based borosilicate glass showed broad emission spectra of the 1.55μm transition and large Ω_6 of Er^{3+} ion[4)]. In 2001, a group of Corning reported the MCS (multi-component silicate) glass containing Sb_2O_3, which shows wider gain than the glasses[5)]. The important factor dominating the cross section and its bandwidth is the Judd-Ofelt Ω_6 parameter of Er^{3+} ions[6)] as well as the refractive index. We also reported a strong correlation between the Ω_6 and the ionicity of Er-ligand bond in various glasses and its origin[7,8)]. Therefore, it is interesting to investigate glass systems giving ionic ligand fields, which would attain a large Ω_6.

In the first part of this paper, we report the optical properties of the oxide glass based on Sb_2O_3, in which Er^{3+} ions show very broad emission and the local structure of rare-earth ion in this glass. In the second part, possibility of U-band amplifier based on oxide glass ceramics is discussed and an example of Er:YAG glass ceramics is presented. The origin of energy level splitting of $^{2S+1}L_J$ multiplets of rare earth ions should be considered for spectral design. In the third part, we report spectroscopic studies on Tm-doped oxide glasses for an S-band amplifier[P21]. At present, a fluoride fiber based TDFA is practically developed for S^+-band amplifier. However, the chemical durability, long-term reliability of fluoride fiber is an issue to be solved. Also, the gain spectrum of Tm-doped fluoride fiber is a little bit narrow and there exists a gap between the C-band, which is covered by EDFA. We propose that the tellurite glass can be a more practical material.

2. Background

Optically or magnetically active rare earth (RE) ions are characterized by their 4f electrons in seven 4f-orbitals. In addition to the most stable electronic configurations (ground state), various configurations with excited higher energy are possible in the thirteen RE ions from Ce^{3+} to Yb^{3+} ion. The energy of these different electronic configurations is separated by the Coulomb interaction, the spin-orbit interaction and the ligand field interaction,

Email address: stanabe@gls.mbox.media.kyoto-u.ac.jp

resulting in the well-known energy level structures. The electronic transition generally becomes possible between most energy levels, the wavelength of which varies from ultraviolet to mid-infrared regions. It is a fundamental feature of rare earth ions that are utilized as a luminescent centers in many phosphor and laser materials. The wavelength of one of transitions in the Er^{3+} energy level happened to be about 1.55μm: the telecommunication wavelength of optical fibers.

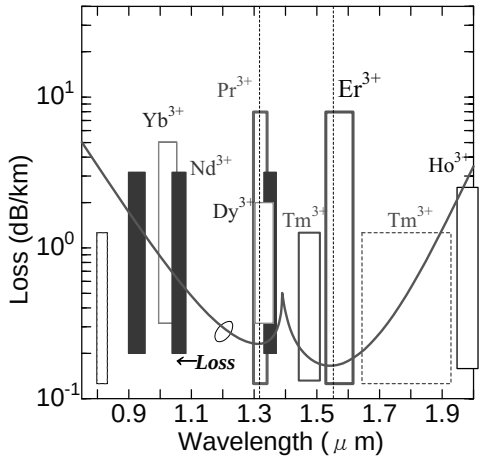

Fig.1. Loss characteristics of silica fiber and emission bands of some rare earth ions.

3. Er-Doped Sb_2O_3-Glasses

3.1. Preparation and Characterization

Glasses in the composition of xSb_2O_3-$3Al_2O_3$- (97-x) SiO_2 (x=27,37,47,57,67) doped with 0.5mol% Er_2O_3 and those doped with 0.5mol% Eu_2O_3 were prepared by melting mixed powders in an alumina crucible at 1100~1450℃. The obtained glasses were cut into 15x10x3 mm^3 shape before polishing into optical surface.

Emission spectra were measured by using a 970nm laser diode (LD) and an InGaAs photodiode (160kHz). The lifetime of the 1.53μm emission was measured by pumping with light pulses of the LD and the time evolution of the signal of the detector was collected with a 100 MHz digital oscilloscope. Decay curves were analyzed by a least-square fitting to get the lifetime.

The number of Er^{3+} ions in unit volume, ρ_N was calculated with the molecular weight and density. Density of the obtained glass was measured by the Archimedes method using kerosene as an immersion liquid. The refractive index, $n(\lambda)$ was measured by a prism coupling method at wavelength of 633nm, 1304nm and 1550nm. Absorption spectra were measured in 400nm ~ 1700nm with Shimadzu UV-3101PC spectrophotometer. With an integrated area of the absorption band, spontaneous emission probability, A of the 1.5μm was calculated by,

$$A(J \rightarrow J') = \frac{(2J+1)8\pi cn^2}{(2J'+1)\bar{\lambda}^4} \times \int_{1.4\mu m}^{1.7\mu m} \frac{k(\lambda)}{\rho_N} d\lambda \quad (1)$$

where c is the light velocity, $\bar{\lambda}$ is the mean wavelength of emission, J and J' are the total momentum for the upper and lower levels, $k(\lambda)$ is the absorption coefficient, and n was the refractive index at wavelength of 1530nm.

The Judd-Ofelt parameters of Er^{3+} ions were calculated by the method described elsewhere[9] with cross sections of five intense bands ($^4F_{7/2}$, $^2H_{11/2}$+ $^4S_{3/2}$, $^4F_{9/2}$, $^4I_{11/2}$, $^4I_{13/2}$) in 470nm ~ 1700nm.

The excitation spectra of the $^5D_0 \rightarrow {}^7F_2$ emission at 613nm of Eu^{3+} doped glasses was measured in the range of 440 ~ 470 nm. The phonon sideband associated with the pure electronic the $^5D_2 \leftarrow {}^7F_0$ transition 465nm was multiplied by 50 times to investigate the phonon mode coupled to rare-earth ions[10], which contributes to multiphonon relaxation.

3.2. Properties of Glass and Spectroscopy of Rare Earth Ions

Fig.2 shows the compositional dependence of refractive index, $n(\lambda)$ of the glasses at 633nm and 1550nm increased with decreasing wavelength. The n of the xSb_2O_3-$3Al_2O_3$-(97-x) SiO_2 glasses (in mol%) at 1.55μm was 1.66~1.90, which increased with increasing Sb_2O_3 content.

Fig.3 shows emission spectra of the $^4I_{13/2} \rightarrow {}^4I_{15/2}$ of Er^{3+}

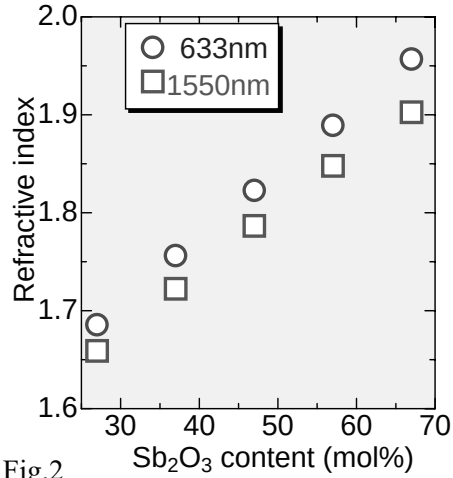

Fig.2 Composiotional dependence of refractive index in xSb_2O_3・(97-x)SiO_2・$3Al_2O_3$・$0.5Er_2O_3$ glasses

ions in the xSb_2O_3-$3Al_2O_3$-(97-x) SiO_2 glasses, in the $75TeO_2$-$20ZnO$-$5Na_2O$-$0.5Er_2O_3$ and in the $95SiO_2$-$5GeO_2$-$0.5Er_2O_3$ as a reference. The spectrum of the silica shows the narrowest bandwidth of about 30nm and that of the tellurite was 60nm-width. It is seen that the Sb_2O_3-based glasses show spectra comparable or broader than that of the tellurite. Fig.4 shows the compositional dependence of fluorescence lifetime, τ_f of the $^4I_{13/2}$ level in the xSb_2O_3-

$3Al_2O_3$-(97-x) SiO_2-0.5 Er_2O_3 glasses. In the range of Sb_2O_3 content x=37-67, the fluorescence lifetimes of the $^4I_{13/2}$ level were almost unchanged, and about 2.5ms, whereas in the Sb_2O_3 content x=27, the lifetime was dramatically decreased.

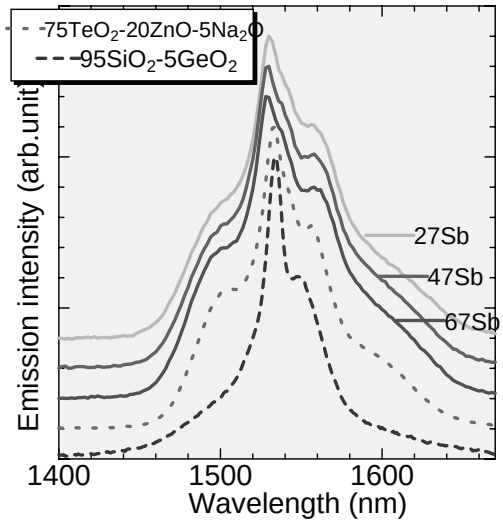

Fig.2. Fluorescence spectra of xSb_2O_3 ・$(97\text{-}x)SiO_2$・$3Al_2O_3$・$0.5Er_2O_3$ glasses.

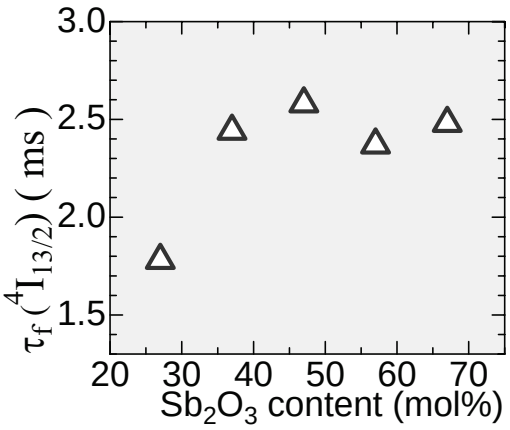

Fig.4 Compositional dependence of lifetime of Er^{3+}: $^4I_{13/2}$ level in glasses.

The excitation spectrum associated with the Eu^{3+}: $^5D_2 \leftarrow {}^7F_0$ transition for the xSb_2O_3- $3Al_2O_3$-(97-x) SiO_2-0.5 Er_2O_3 glasses are shown in Fig.5. The intense band due to the pure electronic transition (PET) Eu^{3+}: $^5D_2 \leftarrow {}^7F_0$ transition is located around 464nm, while the phonon sideband (PSB) coupled to the rare earth ions is observed in the higher-energy range[10]. The position and shape of the phonon sideband were almost unchanged with Sb_2O_3 content.

3.3. Local Structure of Rare Earth Ions in Sb_2O_3-Glass

Fig.6 shows the calculated spontaneous emission probability, *A* of the $^4I_{13/2} \rightarrow {}^4I_{15/2}$ in the xSb_2O_3- $3Al_2O_3$-

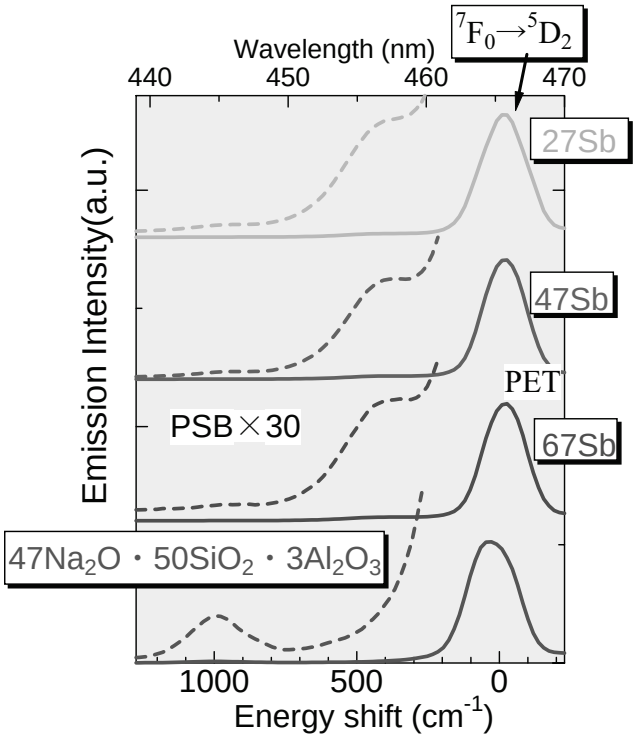

Fig.5. Excitation spectra of Eu^{3+}-doped glasses. Phonon sideband can be observed in the higher-energy- side of $^5D_2 \leftarrow {}^7F_0$ transition.

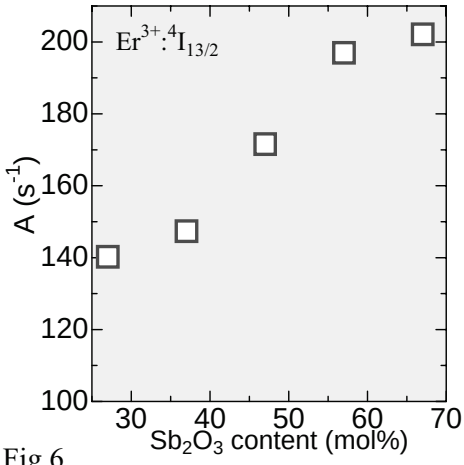

Fig.6 Composiotional dependence of spontaneous emission rate of Er^{3+}:$^4I_{13/2}$ in xSb_2O_3-$(97\text{-}x)SiO_2$-$3Al_2O_3$-$0.5Er_2O_3$ glasses.

(97-x) SiO_2-0.5 Er_2O_3 glasses. The *A* also increased with increasing x, being nearly 200 s^{-1}. The large *A* is mainly due to large *n* of the host glasses, which are composed of large amount of Sb^{3+} ion, a *p*-block element of $5s^2$ electrons having large polarizability [11].

With the measured lifetime and $A_{JJ'}$ from Eq.(1), radiative quantum efficiency, η, were calculated by

$$\eta = \frac{\sum A}{\sum A + \sum W_{NR}} = \tau_f \sum A \qquad (2)$$

and plotted in Fig.7. Reflecting the compositional variations of $A_{JJ'}$, the η increases with increasing Sb_2O_3 content, x. The η values are relatively small compared with those of EDFA's ever reported, but still much larger than that of Pr-doped fiber amplifiers (4%), which perform large gain at 1.3μm[12]. These low values obtained may be due to lower estimation of real local refractive index, i.e., deviation from measured average index. This can be related with no compositional dependence of the local phonon energy obtained from phonon sideband spectra.

Fig.8 shows the compositional dependence of the Judd-Ofelt parameters obtained by using the five electric-dipole bands. It is seen that the Ω_6 values were almost unchanged with Sb_2O_3 content. These results suggest that the Er^{3+} ions are surrounded selectively by Sb_2O_3-rich phase. Generally the A of the $^4I_{13/2}$-$^4I_{15/2}$ band is related with the line strengths, S of electric-dipole (ED) and magnetic-dipole (MD) components by[13],

$$A_{JJ'} = \frac{64\pi^4 e^2}{3h(2J'+1)\lambda^3}\left\{\frac{n(n^2+2)^2}{9}\times S_{JJ'}^{ED} + n^3 \times S_{JJ'}^{MD}\right\} \quad (3)$$

where e is the elementary charge, h is the Planck constant. The MD transition is independent of the ligand field and

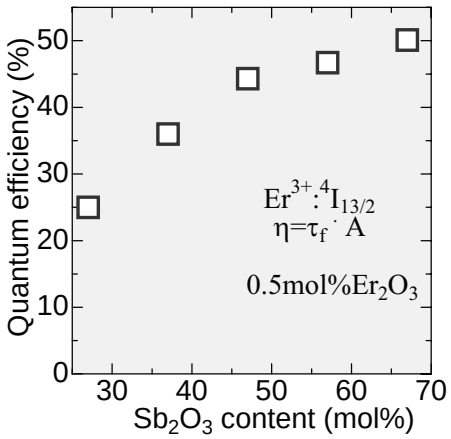

Composiotional dependence of quantum efficiency of Er^{3+}:$^4I_{13/2}$ in xSb_2O_3-(97-x)SiO_2-3Al_2O_3-0.5Er_2O_3 glasses.

contributes to a sharp central peak of spectra around 1.53μm. Because the S^{MD} is characteristic only to the transition determined by the quantum numbers[14], one of the important factors affecting the compositional variations of the emission properties is the ED transition. The S^{ED} of the $^4I_{13/2}$-$^4I_{15/2}$ is obtained with the Judd-Ofelt parameters and reduced matrix elements by[15),16],

$$S^{ed}[^4I_{13/2};^4I_{15/2}] = 0.019\Omega_2 + 0.118\Omega_4 + 1.462\Omega_6 \quad (4)$$

According to Eq.(4), the Ω_6 plays the most dominant role on the cross section of the 1.5μm band among three Ω_t's. Thus in order to increase the bandwidth of spectra, which is varied with local structure, the increase of the Ω_6 would be effective, because the ED contributes to broader component of the 1.5μm band[16]. The large Ω_6 value and refractive index may contribute to broad bandwidth in these glasses.

Fig.9 shows the compositional dependence of the phonon energy, hω obtained from the wavelength of the phonon sideband and that of the pure electronic transition.

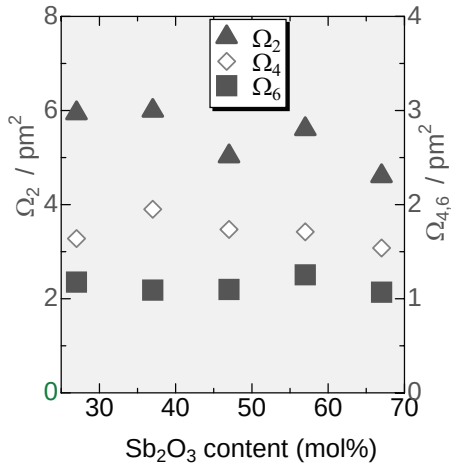

Fig.8. Composiotional dependence of Judd-Ofelt Ω_t parameters of Er^{3+} ions

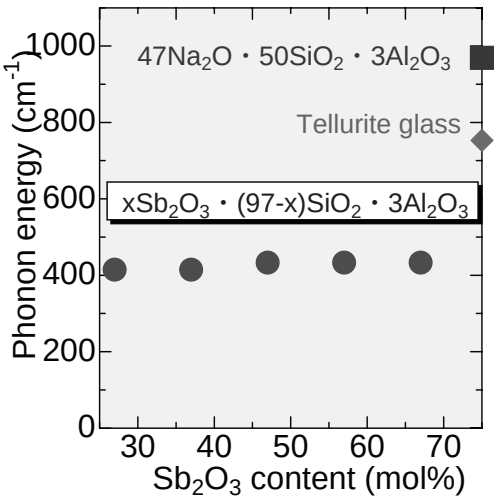

Fig.9. Composiotional dependence of vibration phonon energy from PSB spectra.

The phonon energy was found to be about 400cm^{-1} in all the compositions up to 70mol% SiO_2 content. Usually in most silicate glasses, the Si-O stretching mode is coupled to the rare earth ions even in low SiO_2 composition. The present results are in contrast to the above facts and thus suggest that the Er^{3+} ions are surrounded selectively by Sb_2O_3-rich phase and are not affected by Si-O with about 1000cm^{-1} energy

3.4. Origin of "Non-silicate" environment

Fig.10 show the TEM image and a structural model of the glass, where the nano-scale phase separation can be observed. The dark region can be Sb_2O_3-rich phase and the other can be SiO_2-rich phase. Since the solubility of rare earth ions in a pure silica or silica-rich glass is very low[17], Er^{3+} ions can be condensed in the Sb_2O_3-rich phase, as indicated in the spectroscopic results mentioned above. The concentration dependence of lifetime of Er^{3+}:$^4I_{13/2}$ shows more rapid decrease in a Sb_2O_3-poor composition, indicating that Er^{3+} ions are more condensed. The tendency is moderate in glasses with Sb_2O_3-rich compositions.

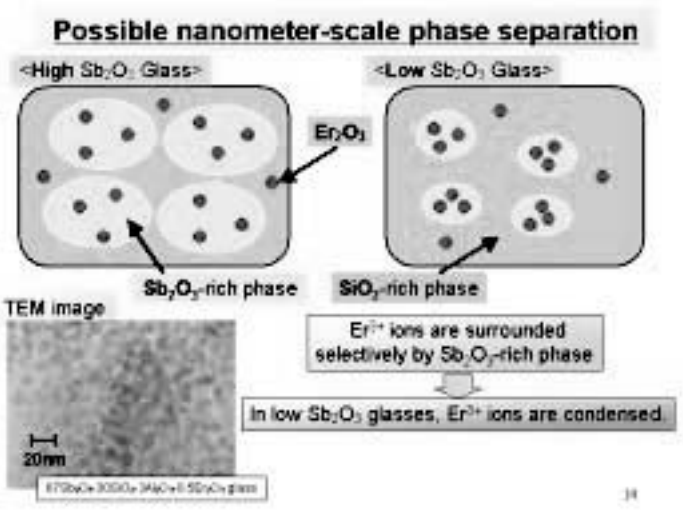

Fig.10. TEM image of the glass and a structural model of nano-scale phase separation.

4. Potential Materials for U-band Amplifier

4.1. Rare earth candidates for 1.6μm emission

Two rare earth ions have been reported to show emission in the U-band wavelength range. Choi reported 1.6μm emission for the Pr^{3+}:$^4F_{3,4}\rightarrow{}^3H_4$ in a selenide glass[18] and Lee reported the Ho^{3+}:$^5I_5\rightarrow{}^5I_7$ transition in a sulfide glass[19]. Fig.11 shows the energy level diagrams of candidate ions with 1.6μm transition[P22]. As can be seen from Fig.11, the energy gap of the Pr^{3+}:$^4F_{3,4}$ and Ho^{3+}:$^5I_5$ are 1400 cm^{-1} and 2500cm^{-1}, respectively. The gain efficiency of amplifiers is dominated by the quantum efficiency of the initial level, which is largely dependent on the multiphonon decay loss. For the levels with the energy gap to the next lower level, ΔE is 3000cm^{-1}, oxide glasses with phonon energy, hω, higher than 600cm^{-1} cannot be a practical host with good efficiency, because the multiphonon decay rate, W_p increases drastically when ΔE/hω is less than 5. In the case of U-band emissions for Pr^{3+} and Ho^{3+}, even the phonon energy of typical fluoride glasses such as ZBLAN (~500cm^{-1}) is too high to suppress the nonradiative loss. That is the main reason why the 1.6μm emission is reported only in chalcogenide glasses, hω of which is less than 400cm^{-1}. However, the fiberizability and reliability of nonoxide glasses are issue for practical application. On the other hand, ΔE of the Er^{3+}:$^4I_{13/2}$ is 6500cm^{-1}, large enough to obtain quantum efficiency over 90% even in oxide hosts with high phonon energy.

4.2. Do we really know spectra of Er^{3+}?

In addition to the C-band and L-band EDFA, the S-band EDFA was reported in a conventional silica-based EDF[20]. It requires a special and tricky pumping configuration with several C-band ASE-suppression filters and much higher pumping power is required than normal EDFAs for the C+L band. Due to the energy distribution, mainly to the Stark level structure of major Er^{3+} ions in glasses, most of glass-based EDFAs usually cover only C+L-band (1520~1610nm) by normal pumping scheme.

Fig.12 shows the origin of spectral broadening due to energy level splitting of $^{2S+1}L_J$ state of lanthanide ions in crystalline ligand field and in disorderd solids. In a crystalline host, depending on its structure, a unique ligand

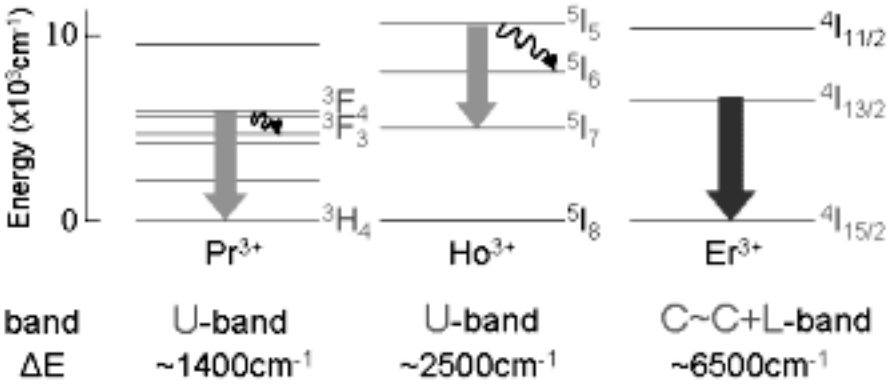

Fig.11 . Energy level diagrams of Pr^{3+}, Ho^{3+}, and Er^{3+} ions. The energy gap of the initial level of 1.6μm emission is also shown.

field can be expected for anomalous Stark splitting. Possibility of homogeneous doping of Er^{3+} ions in crystals is determined by the availability of crystallographic sites suitable for lanthanide substitution. Crystals composed of Y^{3+}, La^{3+} or Gd^{3+} ions, such as yttrium aluminum garnet, YAG, can accommodate substantial amount of other optically 4f-active lanthanide ions in the rare earth site. The spectral shape of doped crystals usually become discrete, while those of doped glasses are continuously broadened. The spectral features of glasses are advantageous for obtaining a flat gain spectrum as a WDM amplifier, but we might not be able to expect anomalous Stark splitting for Er^{3+} ions, since the absence of structural restriction of the crystallographic site in glass may usually result in well-observed "averaged" spectrum centered at 1530nm.

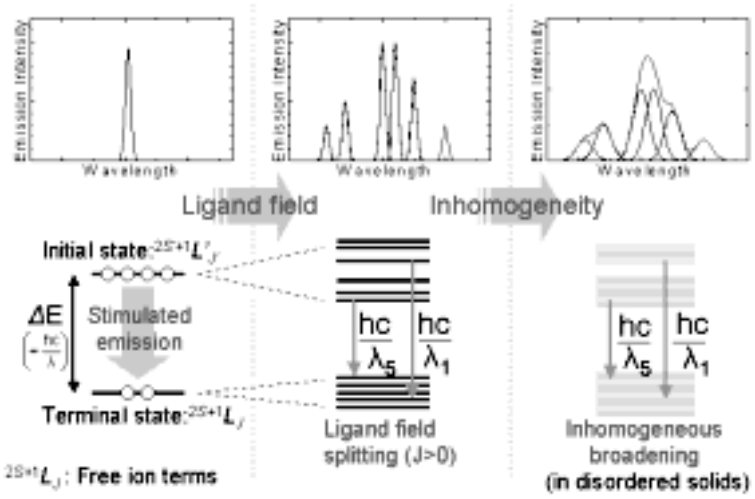

Fig.12 Origin of spectral broadening due to energy level splitting of $^{2S+1}L_J$ state of lanthanide ions in crystalline ligand field and in disordered solids.

4.3. Line Broadening in Er:YAG Glass Ceramics

In 2003, we have reported the U-band emission in a glass ceramics containing Er:YAG [P22]. Fig.13 shows the comparison of Er^{3+}: $^4I_{13/2} \rightarrow {}^4I_{15/2}$ emission in glasses and YAG crystal. Due to its unique Stark level structure, the emission bands are observed in the U-band range. Sharp spectral bands can be moderated by introducing inhomogeneity to the Y^{3+}-site in disordered structure by means of formation of solid solution. The $Ca_3Al_2(SiO_4)_3$ crystal has a cubic garnet structure, the lattice constant of which is only 1% different (a_0=11.849A) from that of cubic YAG (a_0=12.009A). Solid solution can be formed in the composition $Y_{3-x}Ca_xAl_{5-x}Si_xO_{12}$. Charge neutrality is maintained by substitution of same amount of Y^{3+} and Al^{3+} with Ca^{2+} and Si^{4+} at octahedral and tetrahedral sites, respectively. Er^{3+} ions can substitute the Y^{3+} site, the structural configuration of the second nearest cations around which can be varied in the solid solution. This variation results in variation of the ligand field based on the eight nearest oxygen ions and thus can lead to the inhomogeneous broadening of spectra. Our glass ceramics is a CaO-Y_2O_3-Al_2O_3-SiO_2 system, in which the Er:YAG phase contains a certain amount of Ca^{2+} and Si^{4+} [P22]. As shown in Fig.14, the emission spectra of the glass ceramics are slightly broadened compared with that of Er:YAG crystal. More detailed studies are necessary to clarify the effect of nano-sized crystals and solid solution on the inhomogeneous broadening of emission spectra [P4].

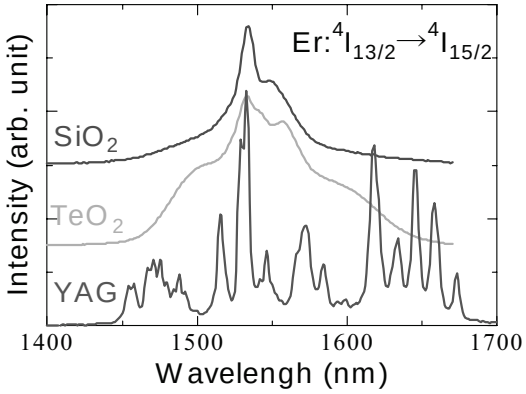

Fig.13. Emission spectra of Er^{3+} in glasses and YAG crystal.

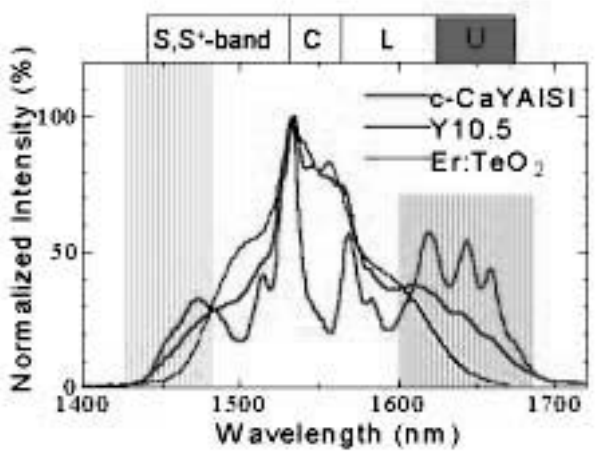

Fig.14. Emission spectra of Er:YAG glass ceramics and a tellurite glass.

5. Tm-doped glasses for S-band amplifier

5.1. Optical Transitions in Tm^{3+} ion

Because the silica-based transmission fiber has a wide window from 1.4μm to 1.65μm, there is emergent demand for optical amplifiers, which can be used around 1.4μm and 1.6μm, in addition to the present silica-based Er-doped fiber amplifiers (EDFA). Tellurite-based EDFA was reported to have 80nm-wide gain up to 1.6μm (L-band), which also shows various excellent material properties[3]. For the 1.45～1.49μm band (S^+-band), the fluoride-based Tm-doped fiber (TDF)[21] can be used as an amplifier, although it still presents difficulties compared with the use of EDFA. One of the reasons for inferior performance of TDFA is the longer lifetime of the terminal $^3F_4$ level than that of the initial $^3H_4$ level[22]. The performance of the TDFA is improved by use of an upconversion-pumping scheme with a 1.06μm laser, which produces a population inversion[22]. Codoping of other lanthanide ion, such as Ho^{3+}, was also found to improve the population inversion by means of the energy transfer from the $^3F_4$ level[23]. In addition, a larger branching ratio, β of the $^3H_4 \rightarrow {}^3H_6$ band at 0.80μm than that of the 1.45μm make it difficult to realize amplification, because the fiber can easily lase at 0.80μm, resulting in the gain saturation[24]. According to the Judd-Ofelt calculation, β of 0.80μm is nearly 90%, which is 11 times larger than that of 1.46μm emission in most glasses[25,26]. Therefore, the suppression of the 0.80μm amplified spontaneous emission (ASE) is important to avoid lasing at unexpected wavelength for improving the amplifier performance. In either case, in spite of difficulty as practical materials, non-oxide fiber hosts with lower phonon energy have been used, because the $^3H_4$ level is more easily quenched in high-phonon-energy environment due to its small energy gap. However, the energy gap of the $^3H_4$ level is not so small as that of the Pr:$^1G_4$ for 1.3μm amplifiers and thus good performance can be expected in some oxide hosts with low phonon energy and better fiberizability.

In this study, the tellurite glass was chosen as a host because it has relatively low phonon energy, excellent properties for fiber fabrications[3),27)[P21}] and thus considered as a candidate material for TDFA.

5.2. Glass preparation and measurements

Glasses in the composition of $72TeO_2$-$20ZnO$- $5Na_2O$-$3Ln_2O_3$ (3Ln=(3-x)Y+xTm, (2.9-y) Y + 0.1Tm + yHo, Tb, or Eu) were prepared. High-purity (99.999%) starting oxide and carbonate materials were mixed and melted in a gold crucible at 900℃ for 45 minutes, then poured into preheated stainless-steel molds and annealed around glass transition temperature for 2 hours. The samples were cut and polished into 10x10x2mm^3.

Absorption spectra were measured with a Shimadzu UV-3101PC Spectrophotometer in the range of 300~2200 nm. The Judd-Ofelt analysis was done with absorption cross sections of four electric- dipole transitions to obtain three Ω_t parameters (t=2,4,6), which were used to calculate the spontaneous emission probabilities, *A* and the branching ratios, β from the $^3H_4$ level.

Emission spectra were measured by using a 792nm laser diode, LD, (Sony 304XT) and a monochromator (Nikon-G250) from 700nm to 2300nm. InGaAs and PbS photodiodes were used as a detector. The sensitivity calibration of this measurement system was done with the spectra of a standard halogen lamp to evaluate the branching ratio of bands of Tm^{3+} at separated wavelengths. For the lifetime measurement, the LD was electrically modulated to get short pulses and the luminescence decay curves were recorded with a digital storage oscilloscope (LeCroy, LS140, 100MHz) to calculate the lifetime by least-square- fitting with a single or double exponential function. In the fluorescence measurement the sample temperature was controlled from 15K to 300K with a helium-cycling cryostat (Iwatani Plantec Co., TCU4).

5.3. Spectroscopy of Singly Doped Glass

5.3.1. Fluorescence spectra

Figure 15 show the Tm^{3+} energy level and related fluorescence transitions, excited by 790nm. The emission bands at 0.80μm, 1.46μm, and 1.80μm are due to the $^3H_4 \rightarrow {}^3H_6$, $^3H_4 \rightarrow {}^3F_4$, and $^3F_4 \rightarrow {}^3H_6$, respectively. The wavelength region longer than 1.3μm is multiplied by 30 times. The relative intensity ratio of 0.80μm to 1.46μm was about 11, almost unchanged with glass compositions and Tm-concentration. On the other hand, that of 1.46μm to 1.80μm was largely changed with these factors, which is due to the effect of the nonradiative relaxations.

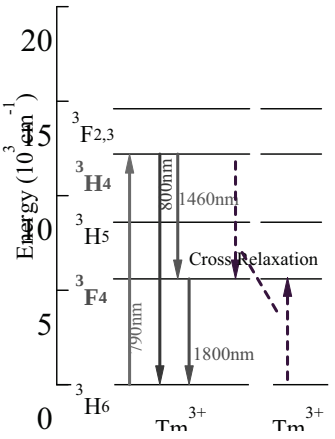

Fig.15. Energy level of Tm^{3+} ion.

5.3.2. Judd-Ofelt analysis and quantum efficiency in tellurite

The obtained Judd-Ofelt parameters of Tm^{3+} in the

present glass were; Ω_2= 4.69pm^2, Ω_4=1.83pm^2, Ω_6 = 1.14pm^2. According to our calculations of spontaneous emission probabilities, *A* and β, from the $^3H_4$ level of Tm^{3+} ions in the tellurite glass, the β of 0.80μm emission is 11 times larger than that of 1.4μm emission, which is almost similar to the case in fluoride and other oxide glasses. The calculated τ_R was 366μs, while the measured lifetime was 350μs. This indicates that the quantum efficiency of the $^3H_4$ level is 96% in tellurite glass, which is comparable to that in ZrF_4-based fluoride glasses (~100%).

5.3.3. Concentration dependence of emission

Figure 16 shows the Tm_2O_3- concentration dependence of ratios of the $\tau_f(^3F_4)/\ \tau_f(^3H_4)$ and the integrated intensity of (1.80 μm)/ (1.46μm) of fluorescence spectra. Both ratios increase drastically with increasing Tm_2O_3 content. These phenomena are well understood by so-called "Two-for-One process" [P21], which is a result of the cross relaxation between two Tm^{3+} ions; $[^3H_4, {}^3H_6]\rightarrow[^3F_4, {}^3F_4]$ and unfavorable for population inversion between the $^3H_4$ and $^3F_4$ levels. Therefore, a low concentration is desirable to keep a high quantum efficiency of the $^3H_4$ level for 1.4μm application.

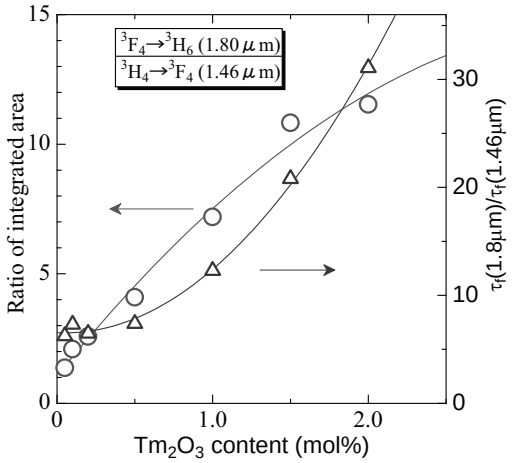

Fig.16. Tm-concentration dependence of ratio of integrated intensity and lifetime of 1.4μm/1.8μm emissions.

5.3.4. Temperature dependence of spectra

Figure 17 shows temperature variation of the fluorescence spectra. The peak intensity of the 1.46μm- band increases with lowering temperature, while the line shape of the 1.8μm-band becomes sharp. It can be seen that the mean wavelength of both bands shift to the longer side. The temperature dependence of integrated intensities of both bands are plotted in Fig.18. The integrated area of the 1.46μm- band is almost unchanged at lower temperature and drops with temperature above 150K. On

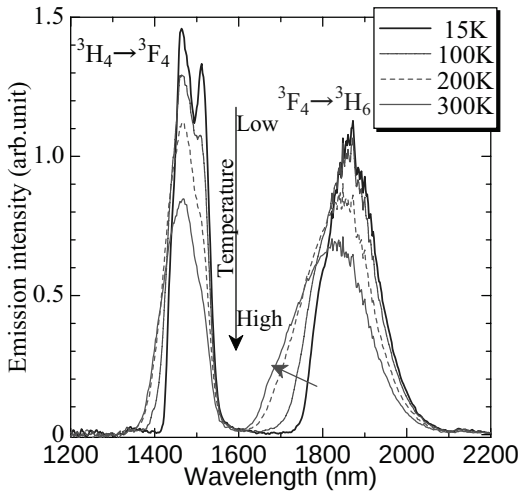

Fig.17. Temperature variation of emission spectra of a Tm-doped tellurite glass

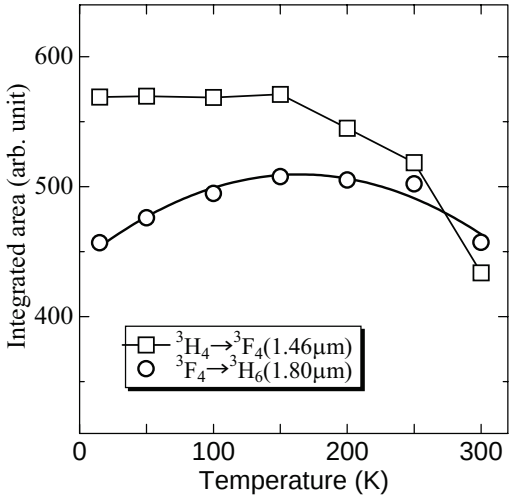

Fig.18. Temperature dependence of emission intensity of 1.46μm and 1.80μm in a Tm-doped tellurite glass

the other hand, that of the 1.8μm-band increases slightly and decreases above 250K. The tendency of the 1.46μm emission can be explained by considering the temperature dependence of the nonradiative decay from the $^3H_4$ level, which has smaller energy gap to the next lower level. The increasing tendency of the 1.8μm-band is ascribed to the improved population from the upper level by nonradiative processes. Therefore, the lower the temperature is, the better the population inversion becomes. Another advantage of the lower temperature can be the much improved intensity at 1.50~1.52μm, which is hardly obtained by conventional EDFA, though not impossible by TDFA[28].

5.4. Effect of Codoping of Ho, Tb, Eu

Several studies on the codoping of other lanthanide ions in the Tm-doped fluoride glass have been carried out by

several authors[25),29-31)]. The role expected for a codopant is to quench the $^3F_4$ level selectively without quenching the $^3H_4$ level. From this viewpoint, the Eu^{3+}, Tb^{3+} and Ho^{3+} can be a candidate among thirteen 4f-active lanthanide ions. The energy level diagrams of these ions are shown in Fig.19.

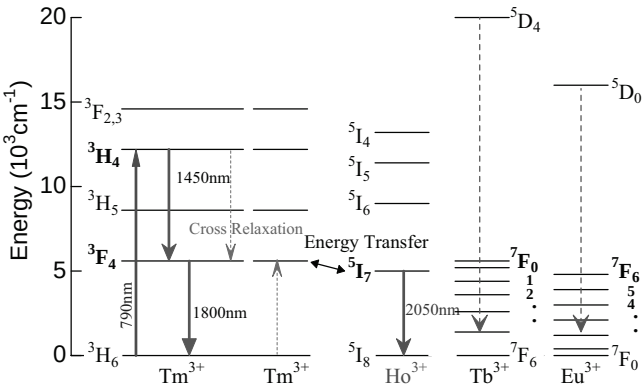

Fig.19. Energy level of Tm^{3+}, Ho^{3+}, Tb^{3+}, and Eu^{3+} ions

The Ln-concentration dependence of the lifetimes of the Tm^{3+}:$^3H_4$ and $^3F_4$ levels are plotted in Fig.20. Among three codopants, the Eu^{3+} ion quenches both levels most significantly and the Ho^{3+} ion shows the best selectivity; i.e., the least effect on the $^3H_4$ lifetime with a large quenching effect on the $^3F_4$.

The variation of the fluorescence spectra of Tm-Ho codoped tellurite glasses are shown in Fig.21. The spectra are normalized by the intensity of 1.46μm-band, because it showed the least change. We see a drastic decrease of the 1.8μm-band and a rapid increase of the

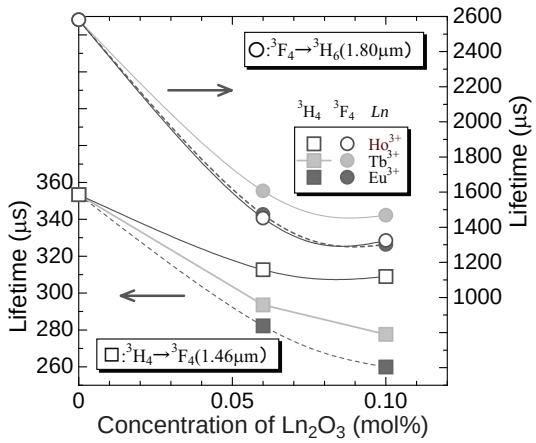

Fig.20. Effect of codopants on lifetimes of Tm-levels in tellurite glasses

Ho^{3+}:$^5I_7$→$^5I_8$ emission intensity at 2μm. This result is an evidence of the Tm:$^3F_4$→Ho:$^5I_7$ energy transfer, which can contribute to the population inversion.

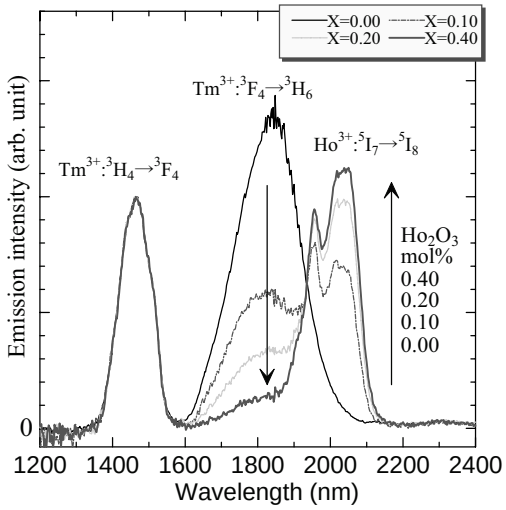

Fig.21. Variation of emission spectra of Tm-Ho-codoped tellurite glasses.

Conclusions

The Sb_2O_3-silicate glasses offers specific local environment to RE ions and shows broad emission spectra of 1.5μm with a large cross section of Er^{3+} ions. It is suggested that the nano-scale phase separation exist in these glasses and the Er ions are selectively condensed in the Sb_2O_3-rich phase. In the YAG-glass ceramics, Er^{3+} ions show U-band emission, the bandwidth of which became broader than that in a bulk crystal. The Tm^{3+}-doped tellurite glasses can be a potential candidate for an S-band amplifier as an oxide glass fiber.

Acknowledgments

The author thanks Mr. T.Tamaoka, M.Nishi, S.Ono, M.Onishi, H.Yamazaki and Y.Kishi, graduate students in Tanabe labs, for their cooperation in this project, although he could not incorporate many of their research results in this paper.

References

1) H.Taga, "High-capacity and long-distance WDM transmission technologies", *1999 Tech.Digest 10th Optical Amplifiers and their Applications*, (OSA, Washington, DC, June 1999) WC1, pp.22-25.

2) J.S.Wang, E.M.Vogel, E.Snitzer, "Tellurite glass: a new candidate for fiber devices", *Opt. Mater.* **3**, 187 (1994).

3) A.Mori, Y.Ohishi and S.Sudo, "Erbium-doped tellurite fiber laser and amplifier", *Electron. Lett.* **33**[10], 863-864 (1997).

4) S. Tanabe, N. Sugimoto, S. Ito, T. Hanada, "Broad-band 1.5μm emission of Er^{3+} ions in bismuth-based oxide glasses for potential WDM amplifier", *J.Luminesc.* **87**, 670-672 (2000).

5) J.Minelly, A.Ellison, "Applications of antimony-silicate glasses for fiber optic amplifiers", *Opt.Fiber Tech.* 8, 123-138 (2002).

6) S.Tanabe, T.Hanada, "Local Structure and 1.5μm quantum efficiency of erbium doped glasses for optical amplifiers," *J.Non-Cryst. Solids*, **196**, 101-105 (1996).

7) S.Tanabe, T.Ohyagi, T.Todoroki, T.Hanada, and N.Soga, "Relationship between the Ω_6 Intensity Parameters of Er^{3+} Ions and The ^{151}Eu Isomer Shift in Oxide Glasses", *J.Appl.Phys.* **73**[12] 8451-54 (1993).

8) S.Tanabe, K.Takahara, M.Takahashi and Y.Kawamoto, "Spectroscopic studies on radiative transitions and upconversion characteristics of Er^{3+} ions in simple pseudo-ternary fluoride glasses MF_n-BaF_2-YF_3 (M: Zr, Hf, Al, Sc, Ga, In, or Zn)", *J. Opt. Soc. Am. B* **12**[5] 786-793 (1995).

9) S.Tanabe, T.Ohyagi, N.Soga, and T.Hanada, "Compositional dependence of Judd-Ofelt parameters of Er^{3+} ions in alkali-metal borate glasses", *Phys. Rev. B* 46 [6], (1992) 3305-10.

10) S.Tanabe, S.Todoroki, K.Hirao, N.Soga, "Phonon Sideband of Eu^{3+} in Sodium Borate Glasses", *J.Non-Cryst.Solids* **122**, 59-65 (1990).

11) W.H.Dumbaugh, "Heavy-metal oxide glasses", *Phys.Chem.Glasses* **27**, 119 (1986).

12) Y. Ohishi and J. Temmyo, "The Status of 1.3μm Fiber Amplifier," *Bull. Ceram. Soc. Japan* **28**, 110-14 (1993).

13) R.D.Peacock, "The Intensities of Lanthanides *f-f* Transition"; pp.83-122 in *Structure and Bonding* , Vol. 22. Ed. by J.D. Dunitz et al., (Springer-Verlag, Berlin, 1975),

14) W.T.Carnall, P.R.Fields, K.Rajnak, "Electronic Energy Levels in the Trivalent Lanthanide Aquo Ions. I. Pr^{3+}, Nd^{3+}, Pm^{3+}, Sm^{3+}, Dy^{3+}, Ho^{3+}, Er^{3+}, and Tm^{3+}," *J. Chem. Phys*., **49**[10], 4424-4442 (1968).

15) M.J.Weber, "Probabilities for Radiative and Non-radiative Decay of Er^{3+} in LaF_3", *Phys. Rev.* **157**[2] 262-72(1967).

16) S.Tanabe, "Optical transitions of rare earth ions for amplifiers: How the local structure works in glass", *J.Non-Cryst.Solids* **259**, 1-9 (1999).

17) K.Arai, H.Namikawa, K.Kumata, T.Honda, H.Ishii, T.Handa, "Aluminum or phosphorus co-doping effects on the fluorescence and structural properties of neodymium-doped silica glass", *J.Appl.Phys.* 59[10], 3430-36 (1986).

18) Y.G.Choi, K.H.Kim, B.J.Park, J.Heo, "1.6μm emission from Pr^{3+}:($^3F_3$,$^3F_4$)→$^3H_4$ transition in Pr^{3+}- and Pr^{3+}/Er^{3+}-doped selenide glasses", *Appl.Phys.Lett*. 78[9], 1249-51 (2001).

19) T.H.Lee, J.Heo, "Spectroscopic properties of Ho^{3+} doped chalcogenide glasses for 1.6μm(U-band) fiber optic amplifier", *Abstract Int'l Sympo. on Photonics Glasses 2002*, 20 (Shanghai, Oct. 2003).

20) E.Ishikawa, M.Nishihara, Y.Sato, C.Ohshima, Y.Sugaya, J.Kumasato, "Novel 1500-nm band EDFA with discrete Raman amplifier", *ECOC2001*, PD.1.1.2, (Amsterdam, 2001).

21) T.Sakamoto, A.Aozasa, T.Konamori, K.Hoshino, M.Yamada, M.Shimizu, "Gain-equalized thulium-doped fiber amplifiers for 1460nm-band WDM signals", *1999 Tech.Digest 10th Optical Amplifiers and their Applications*, (OSA, Washington, DC, June, 1999) WD2-1, pp.50-53.

22) R.M.Percival, D.Szebesta, J.R.Williams, "Highly efficient 1.064μm upconversion pumped 1.47μm thulium doped fluoride fiber laser", *Electron.Lett.* **30**[13], (1994) 1057-58.

23) T.Sakamoto, M.Shimizu, T.Kanamori, Y.Terunuma, Y.Ohishi, M.Yamada, S.Sudo, "1.4-μm-band gain characteristics of a Tm-Ho-doped ZBLYAN fiber amplifier pumped in the 0.8-μm band", *IEEE Photonics Tech. Lett*. **7**[9], (1995) 983-985.

24) T.Komukai, T.Yamamoto, T.Sugawa, Y.Miyajima, "Upconversion pumped thulium-doped fluoride fiber amplifier and lasers operating at 1.47μm", *IEEE J.Quantum Electron*. **31**[11], (1995) 1880-89.

25) S.Tanabe, K.Suzuki, N.Soga and T.Hanada, "Selective sensitization of 480 nm blue upconversion by Tm^{3+}-Er^{3+} energy transfer in tellurite glass", *J.Opt.Soc.Am. **B*** **11**[5], (1994) 933-942.

26) S.Tanabe, K.Tamai, K.Hirao and N.Soga, "Branching ratio of uv and blue upconversions of Tm^{3+} ions in glasses", *Phys.Rev.**B*** **53**[13], (1996) 8358-362.

27) S.Tanabe, T.Kouda and T.Hanada, "Excited energy migration and fluorescence decay in Yb-doped and Yb/Pr codoped tellurite glasses", *Opt.Mater.* **12**, (1999) 35-40.

28) T.Kasamatsu, Y.Yano, H.Sekita, "1.50-μm-band gain-shifted thulium-doped fiber amplifier with 1.05- and 1.56-μm dual-wavelength pumping", *Opt.Lett*. **24**[23], (1999) 1684-86.

29) P.M.Percival, D.Szebesta, S.T.Davey, "Thulium doped terbium sensitized cw fluoride fibre laser operating on the 1.47μm transition", *Electron.Lett.* **29**[12], (1993) 1054-56.

30) S.Tanabe, K.Tamai, K.Hirao and N.Soga, "Excited state absorption mechanisms in red-laser pumped uv and blue upconversions in Tm^{3+} doped fluoroaluminate glass", *Phys.Rev.**B*** **47**[5], (1993) 2507-14.

31) S.Tanabe, X.Feng, T.Hanada, "Improved emission of Tm^{3+}-doped glass for a 1.4μm amplifier by radiative energy transfer between Tm^{3+} and Nd^{3+}", *Opt.Lett.* **25**[11], (2000) 817-819.

Publications

Journal Papers

[P1] S.Tanabe, "Rare Earth Doped Glasses for Fiber Amplifiers in Broad-band Telecommunication", *C.R.Chimie* 5, 815-824 (Dec. 2002).

[P2] S.Tanabe "Properties of Tm-doped tellurite glasses for 1.4μm amplifier", in "*Rare-Earth-Doped Materials and Devices V", SPIE* vol.4282, pp.85-92 (Aug. 2001).

[P3] S.Tanabe, "Design of Rare Earth Doped Amplifiers for WDM Telecommunication", in "Glass Science and Technology on the Threshold of the 3rd Millennium", (ed. W.Pannhorst, Deutschen Glastechn.Gesellschaft, Frankfurt), pp.67-82 (Dec. 2003).

[P4] M.Nishi, S.Tanabe, M.Inoue, M.Takahashi, K.Fujita, K.Hirao, "Fluorescence properties of Er^{3+}-doped YAG nanocrystals synthesized by glycothermal method", *J.Ceram.Soc.Jpn* Suppl. vol.112, S898-S900. (Sept. 2004) .

[P5] S.Tanabe, "Development of Infrared-to Visible Upconverting Rare Earth Doped Glass Ceramics Materials", *Telecom.Frontier* 39, (2003) 29-36 (June 2003).

[P5] S.Tanabe, "Recent trends of Optical Fiber Amplifier for WDM", *Materials Integration* 16[7], 53-59 (July 2003).

[P6] S.Tanabe, "Multi-functional high-performance ceramics: C12A7",

Kagaku 58[5], pp.57-58 (May 2003).

[P7] S.Tanabe, “Development of WDM optical amplifiers by control of 4f-electronic transition probability”, *Kidor*ui 41, pp.1-10 (Nov. 2002).

[P8] S.Tanabe, “Novel oxide glass and glass ceramic materials for optical amplifier”, *Ceram.Trans*. in press (2004).

[P9] S. Tanabe, T. Tamaoka, "Gain characteristics of Tm-doped fiber amplifier by dual-wavelength pumping with a tunable L-band source", *Opt.Mater*. 25[2], 165-169 (Jan.2004).

[P10] S. Tanabe, T. Tamaoka, "Gain characteristics of Tm-doped fluoride fiber amplifier in S-band by dual-wavelength pumping", *J.Non-Cryst.Solids* 326&327, 283-286 (Oct. 2003).

[P11] X.Feng, S.Tanabe, "Spectroscopy and crystal field analysis for Cr(IV) in alumino-silicate glasses", *Opt.Mater*. 20, 63-72 (April 2002).

[P12] T.Tamaoka, S.Tanabe, T.Hanada, "Concentration dependence of emission properties of Tm^{3+}-doped tellurite glasses in telecommunication wavelength region", *J.Ceram.Soc.Japan* 110[4], 325-328 (April 2002).

[P13] T.Tamaoka, S.Tanabe, T.Hanada, "Emission properties of Tm^{3+}-Ln^{3+} (Ho^{3+},Tb^{3+},Eu^{3+}) codoped tellurite glasses by energy transfer", *J.Ceram.Soc.Japan* 110[6], 583-586 (June 2002).

[P14] K.Fukuda, T.Hanada, S.Tanabe, T.Yao, "Physical properties and structure of rf-sputtered amorphous thin films in the system Al_2O_3-Y_2O_3", *J.Am.Ceram.Soc*. 85[4], 915-20 (April, 2002).

[P15] S.Tanabe, H.Hayashi, T.Hanada, "Improved Fluorescence of Tm-Ho and Tm-Ho-Eu Codoped Transparent PbF_2 Glass Ceramics for S-Band Amplifier", *J.Am.Ceram.Soc*. 85[4], 839-43 (Feb.2002).

[P16] S.Tanabe, H.Hayashi, T.Hanada, N.Onodera, "Fluorescence properties of Er^{3+} ions in glass ceramics containing LaF_3 nanocrystals", *Opt.Mater.*19[3], 343-349 (Oct., 2002).

[P17] X.Feng, S.Tanabe, T.,Hanada, "Hydroxyl groups in erbium-doped germanotellurite glasses", *J.Non-Cryst.Solids* 281, 48-54 (April 2001).

[P18] X.Feng, S.Tanabe, T.Hanada, "Spectroscopic properties of erbium-doped ultraphosphate glasses for 1.5μm amplification", *J.Appl.Phys*. 89[7], 3560-67 (April, 2001).

[P19] H. Hayashi, S. Tanabe, and T. Hanada, "1.4μm-band emission properties of Tm^{3+} ions in transparent glass ceramics containing PbF_2 nanocrystals for S-band amplifier", *J.Appl.Phys*. 89[2], 1041-45 (Feb. 2001).

[P20] X.Feng, S.Tanabe, T.Hanada, "Spectroscopic properties and thermal stability of Er^{3+}-doped germanotellurite glasses for broad-band fiber amplifier", *J.Am.Ceram.Soc*. 84[1], 165-171 (Jan.2001).

International conferences

[P21] S.Tanabe, “Properties of Tm-doped tellurite glasses for 1.4μm amplifier”, Proc. SPIE, vol.4282, pp.85-92: "Rare-Earth-Doped Materials and Devices V", (Photonics West, Optoelectronics 2001, San Jose, Jan.23, 2001).

[P22] M.Nishi, S.Tanabe, K.Fujita, K.Hirao, "Novel Er^{3+}-doped glass ceramics with extra-broad emission for S^{+}- and U-band amplifier", *OAA'03*, WC2. *Optical Amplifiers and their Applications 2003*, (Otaru, July 9, 2003)

[P23] S. Tanabe, T. Tamaoka, T. Hanada, Y. Kondo, N. Sugimoto, S. Ito, "Spectral properties of Tm^{3+}-doped glasses for S-band amplifiers", *2001 Tech. Digest Optical Amplifiers & their Applications* (Stresa, July 4, 2001) OWB-4-1-3.

[P24]Y.Kondo, S.Tanabe, N.Sugimoto, S.Ito, T.Hanada, "Ultra-broad band emission of Tm^{3+}-doped bismuth oxide glasses for S-band amplifier", *Ceramics Pac Rim 4 Conference*, (Wailea, Nov.5, '01)

[P25] S.Tanabe, H.Hayashi, T.Hanada, "Fluorescence properties of Tm-doped and Tm-Ho codoped transparent glass ceramics for 1.4 μ m application", *Ceramics Pac Rim 4 Conference*, (Wailea, Nov.5, '01)

[P26] . S.Tanabe, "Design of Rare Earth Doped Amplifiers for WDM Telecommunication", *Proc. Otto-Schott Honorary Colloquim* (German Society of Glass Technology, Jena, Dec.18,2001) vol.74C, 67-82.

[P27] S.Tanabe, T.Tamaoka, "Gain characteristics of Tm-doped fiber amplifier by dual-wavelength pumping with tunable L-band source", *Optical Fiber Communication* 2002, ThZ4, pp.572-574. (Anaheim, March 21, 2002).

[P28] Y.Kondo, T.Nagashima, S.Takenobu, N.Sugimoto, S.Ito, S.Tanabe, T.Hanada, K.Kintaka, J.Nishii, "Fabrication of Bi_2O_3-based Er-doped waveguide for integrated optical amplifier", *Optical Fiber Communication* 2002, TuB4 (Anaheim, March 19, 2002).

[P29] S.Tanabe, "Glass Amplifiers for WDM - History, Recent Progress, Potential", *The First Int'l Workshop on Glass and the Photonics Revolution*”, *Glass Sci.Technol.* 75 C1 (2002) pp.191-210. (invited) (Bad Soden, May 29, 2002).

[P30] S. Tanabe, T. Tamaoka, "Gain characteristics of Tm-doped fluoride fiber amplifier in S-band by dual-wavelength pumping", *Ext.Abstracts XIIth International Symposium on Non-Oxide Glasses and New Optical Glasses*, pp.495-498 (Pardubice, Sept.12, 2002).

[P31] S.Tanabe, "Novel amplifier glasses for broadband WDM telecommunication", Int'l Sympo.Photonics Glasses 2002, (invited) Proc. SPIE Vol. 5061, p. 41-49, International Symposium on Photonic Glass (C.Zhu; Ed. ,Shanghai, Oct.15, 2002).

[P32] S.Tanabe, "Materials and spectroscopy of Tm-doped fiber amplifier" (Invited), Rare-Earth-Doped Materials and Devices VII (Optoelectronics 2003, Photonics West,) 4990-01 (San Jose, Jan.29, 2003).

[P33] S. Tanabe, M. Onishi, K. Hirao, "Optical properties and local structure of Er^{3+}doped antimony silicate glasses for broadband amplifier", 4990-13, “Rare-Earth-Doped Materials and Devices VII” (Optoelectronics 2003, Photonics West 2003, (SanJose, Jan.30, 2003).

[P34] T.Tamaoka & S.Tanabe, "Comparison of gain characteristics of Tm-doped fiber amplifier by different pumping schemes", *OFC2003*, (Atlanta, GA, March 28, 2003).

[P35] S.Tanabe & Y.Kishi, "Optical and physical properties of Tm^{3+} doped germanotellurite glasses for S-band amplifier", *Xth Conference of Physics of Non-Crystalline Solids*, (Parma, July 17, 2003).

[P36] S.Ono, S.Tanabe, "Precise characterization of Er^{3+} ions in fibers with different Al_2O_3 content", *OAA'03*, MD21. *Optical Amplifiers and their Applications 2003*, (Otaru, July 7, 2003).

[P37] T.Tamaoka, S.Tanabe, "Effect of auxiliary L-band laser on the upconversion mechanism of Tm-doped fiber in dual-wavelength pumping scheme", *OAA'03,* MD25. *Optical Amplifiers and their Applications 2003*, (Otaru, July 7, 2003).

[P38] H.Yamazaki, S.Tanabe, "Transparent Cr^{4+}-doped gehlenite($Ca_2Al_2SiO_7$) glass-ceramics for broadband amplifier",

OAA'03, WC1. *Optical Amplifiers and their Applications 2003*, (Otaru, July 9, 2003).

[P39] M.Onishi, S.Tanabe, K.Hirao, "Spectroscopy of Er^{3+} doped antimony silicate glasses for broad-band amplifier", *OAA'03*, WC3, *Optical Amplifiers and their Applications 2003*, (Otaru, July 9, 2003).

[P40] H.Yamazaki, S.Tanabe, "Broadband fluorescence of Cr^{4+} in CaO-Al_2O_3-SiO_2 glasses and novel transparent $Ca_2Al_2SiO_7$ glass ceramics", *The 5th International Meeting of Pacific Rim Ceramic Societies*, 17-O-07 (Nagoya, Sept.29, 2003).

[P41] M.Nishi, S.Tanabe, M.Inoue, M.Takahashi, K.Fujita, K.Hirao, "Fluorescence properties of Er^{3+}-doped YAG nano-crystals synthesized by glycothermal method", *The 5th International Meeting of Pacific Rim Ceramic Societies,* 12-O-25 (Nagoya, Sept. 30, 2003).

[P42] S.Ono, S.Tanabe, "Precise characterization of Er^{3+} ions in silica fibers with difference Al_2O_3 content", *The 5th International Meeting of Pacific Rim Ceramic Societies*, 10-O-07, (Nagoya, Oct.1 2003).

[P43] S.Tanabe, H.Yamazaki, "Transparent Cr^{4+}-doped gehlenite glass ceramics for broadband amplifier", *"Optical Components and Devices"*, Photonics West 2004 (San Jose, Jan.27, 2004).